SHAFT LATERAL AND TORSIONAL VIBRATION RESPONSES TO BLADE(S) RANDOM VIBRATION EXCITATION

B.O. Al-Bedoor*
Mechanical Engineering Department
University of Jordan, P.O. Box 13568, Amman 11942, Jordan

Y. Al-Nassar †
Mechanical Engineering Department, KFUPM Box 1876

L. Ghouti ‡
Information and Computer Science Department, KFUPM Box 1128

and S.A. Adewusi and M. Abdlsamad
Mechanical Engineering Department, KFUPM

الخلاصـــة

تم في هذه الدراسة إعداد تجربة لمراقبة اهتزازات الريش والمحور الدوّار تحت تأثير اهتزازات الرّيش العشوائية. وقد استخدم برنامج العناصر المحدودة (ANSYS) لإيجاد الترددات الطبيعية وأشكالها الاهتزازية للجهاز المُعد لهذه الدراسة. وخلال هذه التجربة، تمّت مراقبة اهتزازات الريش والمحور الدوار بوساطة تثبيت مقاييس الانفعال على الريش والمحور الدوار وعن طريق تثبيت مقاييس تسارعية على حوامل التثبيت ومحطة مقياس الانفعالات الالتوائية للمحور. وقد أظهرت نتائج هذه التجربة أن الاهتزازات الالتوائية للمحور تتأثر بوضوح باهتزازات الريش أكثر من الاهتزازات المقاسة على حوامل التثبيت. وبوجه أخص فإن اهتزازات الريش ذات الترددات المنخفضة تمثـّـل اهتزازات الريش الانحنائية كما أن اهتزازات المحور الالتوائية تمثل الترددات الالتوائية المركبّـة للمحور. وأخيراً فإن نتائج هذه الدراسة تدعم الثقـة في استخدام قياسات الاهتزازات الالتوائية للتعرف على اهتزازات الريش، كما تلقي الضوء في الوقت نفسه على طبيعة التداخل بين الاهتزازات الانحنائية للريش، و الاهتزازات الالتوائية للمحور في حالة الترددات المنخفضة.

* On leave from King Fahd University of Petroleum and Minerals, Dhahran 31261, Saudi Arabia
e-mail: albedoor@ju.edu.jo

† e-mail: ynassar@kfupm.edu.sa

‡ e-mail: ghouti@ccse.kfupm.edu.sa

ABSTRACT

In this study, an experimental set-up for blades-shaft vibration monitoring under blade(s) random vibration excitation is used. The set-up natural frequencies and mode shapes are found using the ANSYS finite element package. The blades and shaft lateral and torsional vibration are monitored using blades strain-gages, bearing accelerometers and shaft torsional strain-gages stations. The results showed that the shaft torsional vibration measurement represents the blade(s) vibration more closely than the bearing accelerometers. In particular, the blades vibration at low frequencies corresponding to the blades bending and shaft torsional coupled modes is closely represented by the shaft torsional vibration signals. The results of this study increased the confidence in using the torsional vibration measurement for blades vibration identification and shed more light on the nature of coupling between the blade bending and shaft torsional vibration that occur at low frequencies.

Key words: Shaft, Torsional, Lateral, Vibration, Strain-Gages, Accelerometer, Coupling, Experimental, Blade(s), Natural Frequencies, Mode Shapes, Random Vibration.

SHAFT LATERAL AND TORSIONAL VIBRATION RESPONSES TO BLADE(S) RANDOM VIBRATION EXCITATION

1. INTRODUCTION

The majority of blades failures in rotating machinery are related to vibration generated fatigue stresses that put growing demands on monitoring blades vibration for design, evaluation, and diagnostics purposes. Blades are attached to the main rotor and interacting with the working fluid which means that they are excited by the working fluid and the main rotor vibrations. This situation makes the vibration measurement process and the identification of blades-related vibration problems a very difficult task. Newly reported and limited studies showed that the main rotor torsional vibration can give the blades vibration signature. An experimental study that shows a comparison between the shaft lateral and torsional vibration measurement under blades random vibration excitation is extremely necessary. Moreover, this experimental study is expected to contribute to the basic understanding of the interaction of blades–rotor systems.

Vibration measurement has been known as a powerful tool in machinery condition monitoring (Laws and Muszynska [1] and Vance [2]), that puts growing demands on developing reliable vibration measuring systems that sense and represent closely the machinery individual component vibration. The main rotor-bearing vibration systems have seen progress and helped in resolving many machinery problems such as the contribution of the eddy current probe in rotor–fluid instability problems. For general-purpose vibration measurement, accelerometers are the most popular vibration pick-ups that collect signals containing all rotor–bearing–housing dynamical behavior. When blades vibration information is required, the task becomes very complicated [3], as the blades are rotating and interacting with the working environment. To directly monitor blade vibration, strain-gages were used in many laboratory-testing studies [4–6]. Other techniques for blades vibration measurement were proposed; among these techniques is the use of Laser-doppler and optical methods [7–9], with some problems and limitations. Detailed discussion of the available methods for blade vibration measurement is reported by Al-Bedoor [10].

The approach of extracting blades vibration frequencies from the shaft torsional vibration was investigated experimentally in references [11–13]. The superiority of this approach to the lateral vibration approach, mainly, arose because torsional vibration is less affected by the boundary conditions than the lateral vibration. Muszynska *et al.* [14] have used the torsional vibration to identify rotor crack. They came up with an explanation for the sensitivity of torsional vibration that damping in torsional vibration modes is minimal. Al-Bedoor *et al.* [15] reported results and discussion of an experimental study on the measurement of blades free and forced vibration using the shaft torsional signals. The results showed that the torsional vibration signal reflect blades vibration up to a certain frequency after which the shaft torsional vibration has less sensitivity to blades vibration. This low sensitivity was related to the experimental set-up limitations and to the idealized single frequency excitation. Although the results of these experiments are promising, there was no comparison between the accelerometer and the shaft torsional vibration signals. Moreover, this study gave no attention to the random vibration of the blades that simulates more closely the fluid induced vibration. A recent theoretical model, Al-Bedoor *et al.* [16], showed that the blade vibration signature can be extracted from the shaft torsional vibration provided that an accurate and sensitive torsional vibration transducer is used. The model provided a tool for evaluating the sensitivity of shaft torsional vibration as related to the blade–disk–shaft combination of properties and what is known as the mistuning effect.

In this work, experimental results on the vibration measurements of rotor lateral and torsional vibration response due to blade random vibration excitation are reported and discussed. A test rig that is compromised of a changeable length shaft, a disk, and four blades has been manufactured. The natural frequencies and mode shapes of the test-rig are found, using the ANSYS finite element package. Strain-gages at two blades to measure blade-bending vibrations and three strain-gage stations are used to measure the shaft torsional vibration. The main rotor lateral vibration is measured using two accelerometers attached to the two bearing housings carrying the rotor. The signals are digitized using LabView and processed using the MATLAB package to find the frequency spectrums.

2. TEST-RIG DESCRIPTION

The test-rig whose schematic diagram shown in Figure 1(*a*) is composed of a rigid stand, two roller element bearings, shaft, and disk holding four blades. The dimensions and material properties of the shaft–disk–blade system are shown in Figure 1(*b*) and listed in Table 1, respectively. Moreover, a photograph that shows the test-rig and the measuring system is given in Figure 2. Three shaft lengths are used, as given in Table 1, to control the system torsional natural frequencies.

As a measuring system, two blades are equipped with full-bridge strain-gage stations located very close to the root of the blade to measure the blade bending vibrations, and three points on the shaft are equipped with a half-bridge strain-gages system at 45° alignment to measure torsional vibrations, as shown in Figure 1(*b*). The five measuring strain-gage stations' results are connected to the signal conditioner (2310 Vishy) that powers the strain-gages, filters for noise signals, and amplifies the signals for further processing. The selected amplifier gain for all five channels is 1000 and the selected filter is the 10 KHz cut off frequency filter. The two accelerometer signals are passed through the conditioning units. The signals are taken to the DAQ of LabView for digitizing and then used in the MATLAB package for analysis. A schematic diagram of the measuring system and signal transmission arrangement is shown in Figure 3.

Table 1. Blade–Disk–Shaft Data.

Property	Value
Blade material	Steel (E=200 GPa, $\hat{\rho}$ = 7850 kg/m^3)
Blade length L	0.125 m
Blade cross section	2.54 × 0.16 cm
Blade mass per unit length, ρ	0.319 kg/m
Blade flexural rigidity, EI	0.173 N.m^2
Disk Material	Aluminum (E = 72 GPA, $\hat{\rho}$ = 2700 kg/m^3)
Disk Radius, R_D	0.06 m
Disk width	0.04 m
Disk mass M_d	1.22 kg
Disk moment of inertia, J_D	2.2×10^{-3} kg.m^2
Steel shaft	G = 80 GPA
Shaft length (three lengths)	L_1 = 83.5 cm, L_2 = 60.5 cm, L_3 = 40.5 cm
Shaft diameter	1 cm
Torsional stiffness k_T with L_1	94 N.m/Rad
L_2	130 N.m/Rad
L_3	194 N.m/Rad

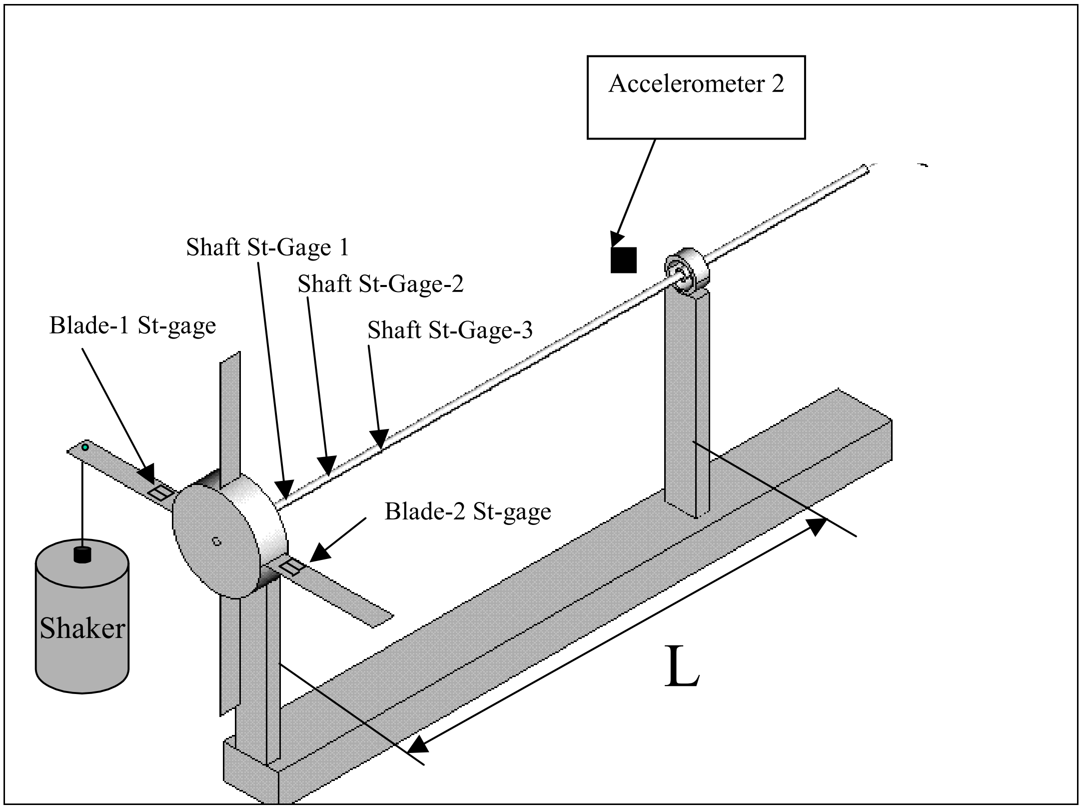

(*a*)

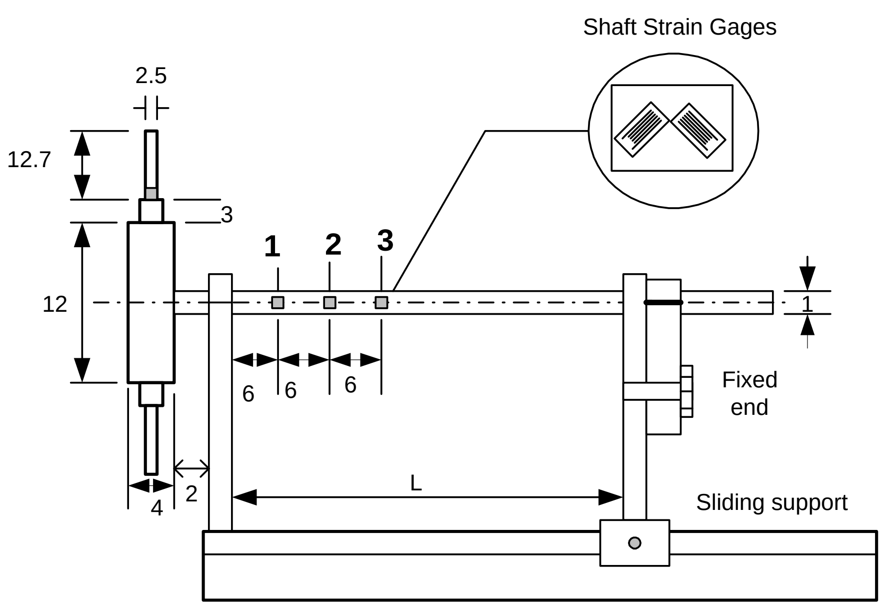

(*b*) DIMENSIONS IN CENTIMETERS

Figure 1. Schematic of the test-rig. (*a*) *general view,* (*b*) *dimensions.*

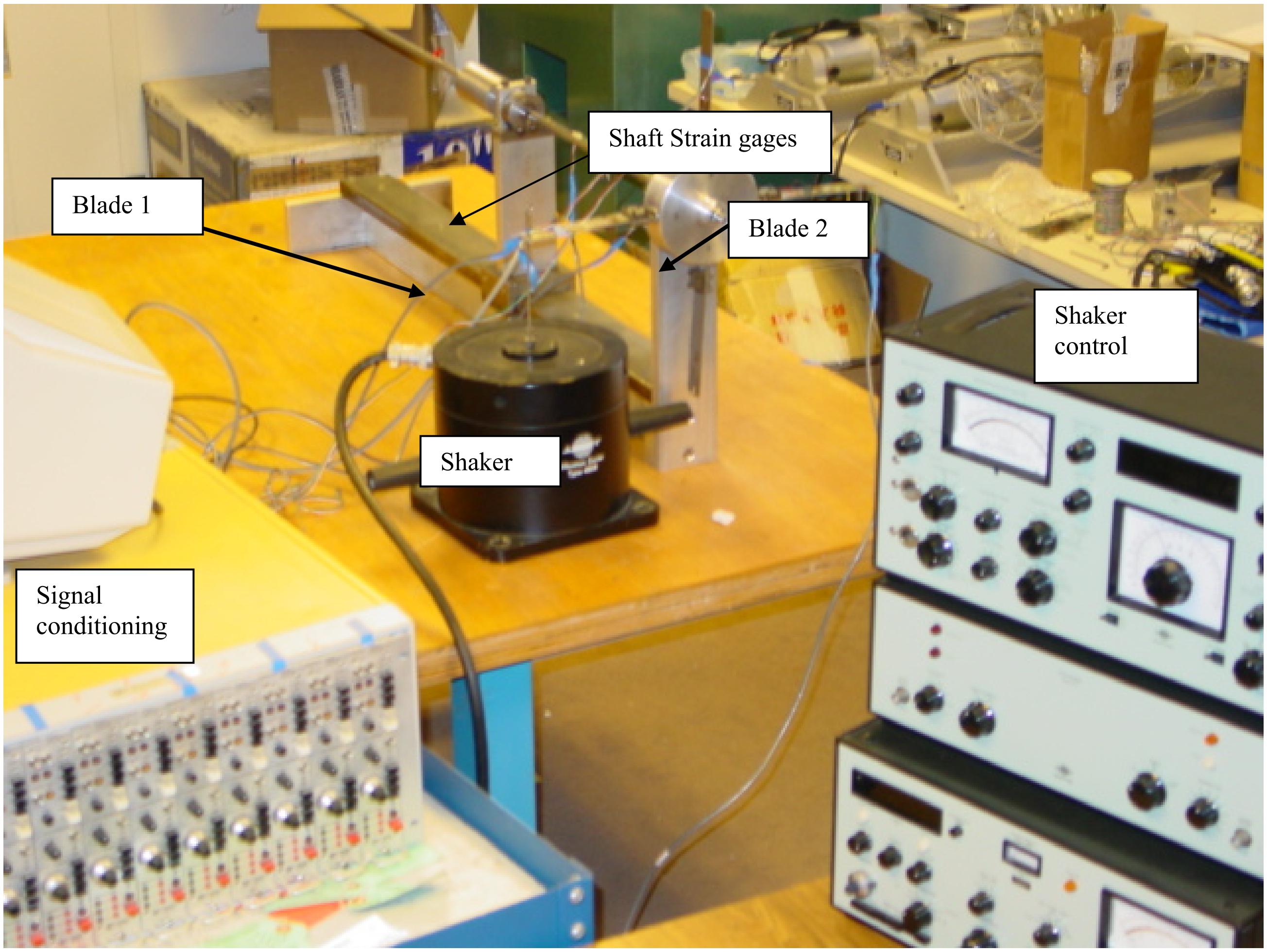

Figure 2. Photograph of the test-rig and measuring system.

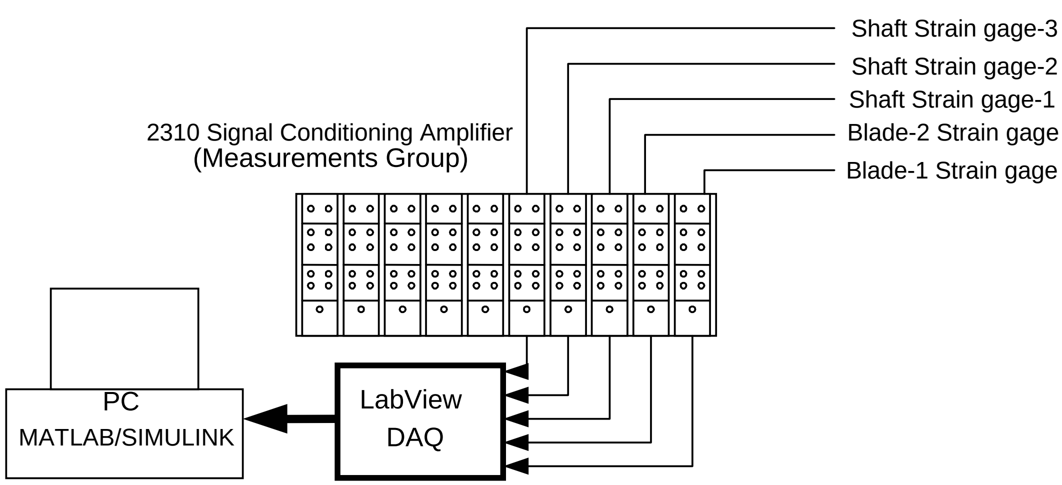

Figure 3. Signal processing diagram.

3. RESULTS AND DISCUSSIONS

In a previous study [15], the blade vibration responses to distinct and sweeping frequency excitation were presented and discussed. This type of excitation represents an idealized condition in which the blade is excited at a single frequency. The more realistic excitation is the one that occurs due to signals with many frequencies, such as the excitation coming from fluid turbulence. Random vibration signals lend themselves to simulate such simultaneous multiple frequency excitations. The excited dynamic system will respond differently according to how close the excitation frequency is to the system natural frequencies. In addition, the random vibration excitation and the measurement of blades, shaft torsional vibration signals, and bearing vibration enable reliable comparison between shaft lateral and torsional vibration signals as measuring tools for the extraction of blade(s) vibration signature.

3.1. Natural Frequencies and Mode Shapes

To identify the experimental set-up natural frequencies and mode shapes, the ANSYS finite element package is used for three different lengths. The calculated natural frequencies are given in Table 2 and the associated mode shapes are given in Figures 4, 5, and 6 for three shaft lengths. As can be seen in Table 2 and Figures 4–6, the assembly has distinct vibration modes, such as the shaft-torsional, shaft-bending, blade-bending, and blade-torsional modes. In addition, the assembly has coupled modes of vibration between the shaft-bending, shaft-torsional, and blade bending.

3.2. Random Vibration Response

For the three different lengths of the shaft, blade 1 is excited by a random white noise shown in Figure 7. The vibration signals from blades 1 and 2, bearing accelerometers, and the three stations for the shaft torsional vibration measurement are collected and their spectrums are studied.

For shaft length $L_1 = 0.835$ m, the vibration spectrums of blades 1 and 2 are shown in Figures 8 (*a*) and (*b*), respectively. As shown in Figure 8(*a*), blade 1 vibration occurs at frequencies of about 3 Hz, 17.5 Hz, 32.5 Hz, 125 Hz, and 300 Hz. Blade 2 spectrum, Figure 8(*b*), shows vibration at 12.5 Hz, 17.5 Hz, 40 Hz, 60 Hz, 75 Hz, and at higher frequencies with lower amplitudes. Now the spectrums of blades 1 and 2 can be considered as characteristic of the set-up blades vibration. The associated accelerometer spectrums are shown in Figures 9(*a*) and (*b*). The accelerometers spectrums show broad band spectrums and no frequency components less than 20 Hz that have the highest amplitudes in the blade spectrums. The shaft torsional strain-gages stations spectrums are shown in Figures 10(*a*), (*b*), and (*c*). The spectrum of strain-gages station 1, Figure 10(*a*), captured vibration at frequencies 20 Hz, 40 Hz, 125 Hz, 180 Hz, 220 Hz, 240 Hz, 260 Hz, 300 Hz, 420 Hz, 440 Hz, and 460 Hz. Torsional strain-gages station 2, Figure 10(*b*), shows vibration at frequencies of 3 Hz, 17.5 Hz, 30 Hz, 60 Hz, 70 Hz, 80 Hz, 120 Hz, 160 Hz, 220 Hz, 240 Hz, 300 Hz, 325 Hz, 340 Hz, 395 Hz, 420 Hz, and 475 Hz. Station 3's spectrum, Figure 10(*c*), shows similar frequencies as station 1 spectrum, as given in Figure 10(*a*). Comparing the spectrums of the torsional stations in Figures 10 indicates that the position of the station makes a difference in the measurement sensitivity. The frequency contents of the five sensors' signals are summarized in Table 3. Considering the frequency content shows that the torsional vibration signals represent the blade(s) vibration more than the accelerometer signals.

Similar spectrums for blades strain-gages, accelerometers and shaft torsional strain-gages are given in Figures 11–13 for the experiment when the shaft length is $L_2 = 0.605$ m. Same behavior of distinct frequencies blade vibration and broad band accelerometers responses can be observed. The shaft torsional vibration signals spectrums, Figures 13, are shown to represent the blades vibration character more closely than the accelerometers spectrums. This observation can be seen in the frequency contents comparison given in Table 4. Towards having more reliable results, the experiment is further conducted for the shaft length $L_3 = 0.405$ m. The spectrums of blades strain-gages signals, accelerometers signals, and shaft torsional strain-gages signals are given in Figures 14–16. The frequency contents of the five spectrums are given in Table 5. Same behavior can be observed as for the former two lengths experiments.

Considering the three experiments on the shaft lateral and torsional vibration measurement under blade random vibration excitation, one can observe the following:

(1) Blade 1 vibrated at distinct frequencies with the highest amplitude at low frequency, which is equivalent to the shaft torsional vibration natural frequency.

(2) Blade 2 vibrated at more frequencies than blade 1 due to its excitation at its base, that produced multiple responses and nonlinear behavior.

(3) Accelerometers showed broad band spectrums and do not represent blade(s) vibration closely. Moreover, accelerometers were not able to sense the blades vibration at low frequencies, even though this low frequency vibration has the highest amplitude.

(4) Shaft torsional vibration measurement showed distinct frequencies and represent blade(s) vibration closely. However, the location of the shaft torsional vibration strain-gages was shown to affect the sensitivity of measurement.

Table 2. ANSYS Simulation Natural Frequencies of the Experimental Setup.

***L* = 0.835 m**		***L* = 0.605 m**		***L* = 0.405 m**	
Frequency Hz	**Mode**	**Frequency Hz**	**Mode**	**Frequency Hz**	**Mode**
2.85	Shaft torsion	2.8606	Shaft torsion	2.87	Shaft torsion
3.8284	Disk tilt	3.8323	Disk tilt	3.8357	Disk tilt
3.8284	Disk tilt	3.8323	Disk tilt	3.8357	disk tilt
27.695	Coupled shaft torsion–blade	23.773	Shaft lateral	12.722	Shaft lateral
43.293	Shaft lateral	23.773	Shaft lateral	12.722	Shaft lateral
43.293	Shaft lateral	27.696	Coupled shaft torsion–blade	27.697	Coupled shaft torsion–blade
63.22	Blade 1st	63.059	Blade 1st	63.182	Blade 1st
63.256	Blade 1st	63.109	Blade 1st	63.22	Blade 1st
63.306	Blade 1st	63.22	Blade 1st	63.232	Blade 1st
71.155	Shaft lateral	79.043	Shaft lateral	79.717	Shaft lateral
71.155	Shaft lateral	79.044	Shaft lateral	79.717	Shaft lateral
131.06	Coupled	148.94	Coupled	147.93	Coupled
131.06	Coupled	148.94	Coupled	147.93	Coupled
166.86	Blade 2nd	166.86	Blade 2nd	166.86	Blade 2nd
237.81	Coupled shaft lateral-blade	210.52	Coupled shaft lateral-blade	223.16	Shaft lateral
237.83	Coupled shaft lateral-blade	210.53	Coupled shaft lateral-blade	223.16	Shaft lateral
370.4	Coupled shaft lateral-blade	369.47	Coupled shaft lateral-blade	338.11	Coupled shaft lateral-blade
370.76	Coupled shaft lateral-blade	369.88	Coupled shaft lateral-blade	338.28	Coupled shaft lateral-blade
385.99	Blade 3rd	385.99	Blade 3rd	385.99	Blade 3rd
392.4	Coupled shaft lateral-blade	393.56	Coupled shaft lateral-blade	390.14	Coupled shaft lateral-blade
393	Coupled shaft lateral-blade	394.11	Coupled shaft lateral-blade	390.93	Coupled shaft lateral-blade
445.53	Shaft lateral	416.84	Shaft lateral	437.16	Shaft lateral
445.53	Shaft lateral	416.84	Shaft lateral	437.16	Shaft lateral
512.45	Blade 4th	512.45	Blade 4th	512.45	Blade 4th
582.66	Coupled shaft lateral-blade	651.16	Blade torsion	651.16	Blade torsion
582.7	Coupled shaft lateral-blade	651.16	Blade torsion	651.16	Blade torsion
651.16	Blade torsion	651.3	Blade torsion	651.32	Blade torsion
651.16	Blade torsion	651.3	Blade torsion	651.32	Blade torsion
651.33	Blade torsion	666.71	Shaft bending	722.39	Shaft bending
651.33	Blade torsion	666.79	Shaft bending	722.39	Shaft bending

Table 3. Frequency Contents for the White Noise Blade Excitation, Shaft Length L_1.

		Frequency contents Hz L_1 White Noise			
Blade 1	Blade 2	Accelerometer	Shaft 1	Shaft 2	Shaft 3
3	12.5	20	20	17.5	20
17.5	17.5	25	125	37.5	105
32.5	37.5	30	185	47.5	125
125	57.5	35	225	55	145
300	75	55	247.5	77.5	187.5
	80	65	307.5	82.5	227.5
	85	75	350	97.5	247.5
	105	80	372.5	102.5	272.5
	125	90	385	125	310
	250	95	432.5	155	350
	335	110	452.5	177.5	372.5
	372.5	120	472.5	185	432.5
	387.5	155		200	437.5
	407.5	180		225	452.5
	430	185		247.5	475
	440	225		285	
	445	285		297.5	
	452.5	300		307.5	
	460	330		315	
		335		330	
		350		335	
		435		347.5	
		440		407.5	
		490		432.5	
				440	
				475	
				485	
				495	

Table 4. Frequency Contents for the White Noise Blade Excitation, Shaft Length L_2.

Frequency contents		Frequency contents L_2 White Noise			
Blade 1	Blade 2	Accelerometer	Shaft 1	Shaft 2	Shaft 3
2.5	5	15	5	20	22.5
20	10	65	22.5	77.5	125
42.5	15	82.5	40	100	142.5
125	20	92.5	105	125	157.5
247.5	42.5	100	125	225	225
305	70	105	145	247.5	245
370	87.5	110	187.5	282.5	307.5
462.5	125	115	210	295	430
500	247.5	122.5	232.5	307.5	457.5
	287.5	135	247.5	322.5	472.5
	297.5	140	252.5	432.5	
	310	150	287.5	500	
	322.5	155	297.5		
	360	287.5	310		
	370	297.5	332.5		
	377.5	307.5	350		
	460	312.5	362.5		
	500	320	372.5		
		325	380		
		330	392.5		
		335	432.5		
		350	475		
		360	485		
		370			
		435			
		445			
		475			
		510			

Table 5. Frequency Contents for the White Noise Blade Excitation, Shaft Length L_3.

		Frequency contents L_3 White Noise			
Blade 1	Blade 2	Accelerometer	Shaft 1	Shaft 2	Shaft 3
2.5	12.5	20	22.5	2.5	22.5
22.5	22.5	25	102.5	22.5	102.5
62.5	55	62.5	125	72.5	125
125	62.5	70	160	82.5	145
150	87.5	87.5	227.5	125	187.5
247.5	125	92.5	247	135	232.5
290	147.5	100	310	147.5	247.5
307.5	282.5	125	352.5	227.5	267.5
352.5	287.5	127.5	392.5	247.5	310
370	300	137.5	435	282.5	352.5
377.5	330	147.5	462.5	287.5	432.5
462.5	337.5	155	475	292.5	462.5
475	352.5	282.5		297.5	475
495	362.5	290		300	
	370	297.5		307.5	
	375	302.5		312.5	
	385	307.5		322.5	
	395	312.5		337.5	
	410	317.5		342.5	
	430	322.5		352.5	
	462.5	330		360	
	497.5	337.5		367.5	
		352.5		377.5	
		370		432.5	
		377.5		447.5	
		450		470	
		470		495	
		500			

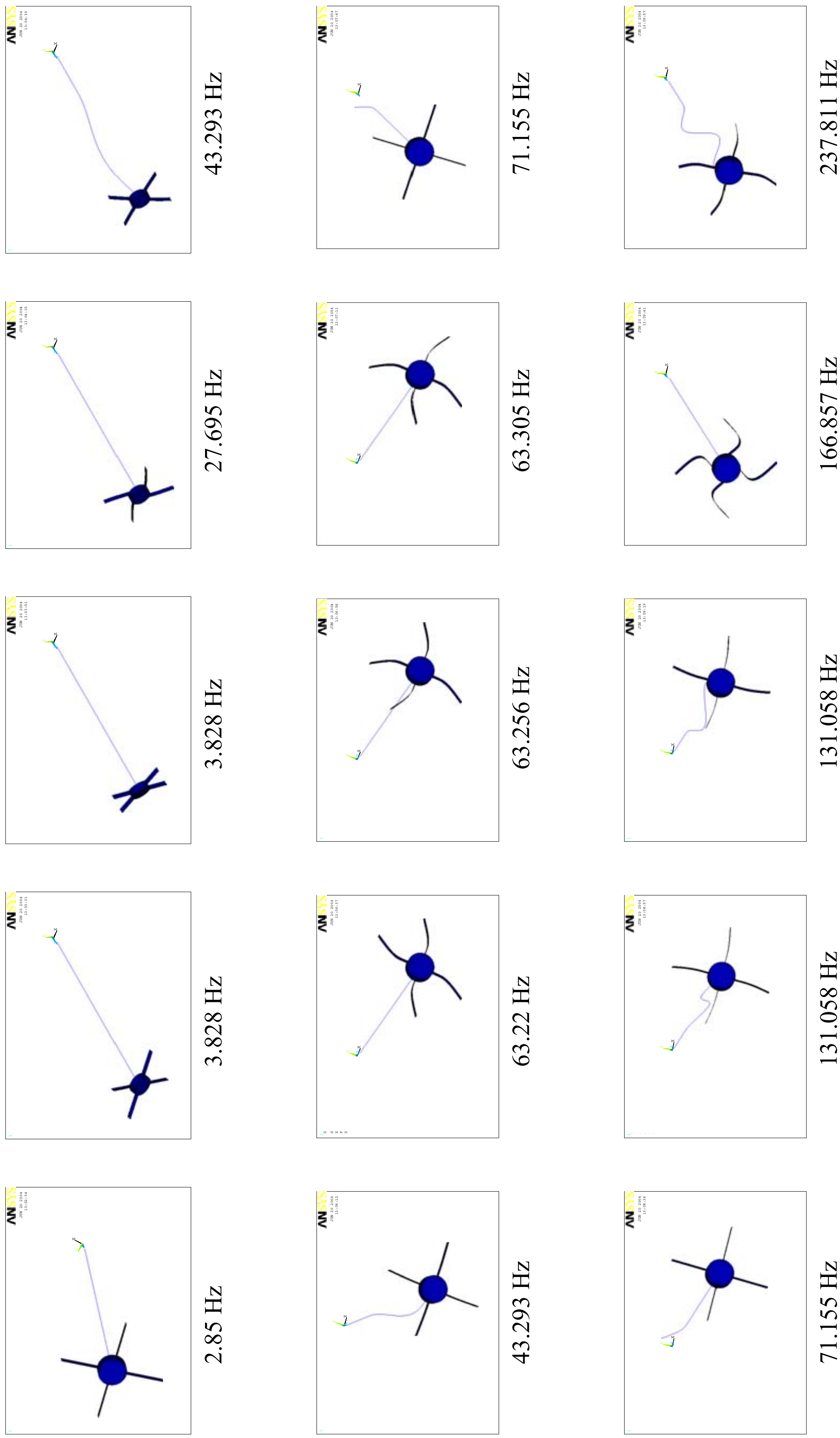

Figure 4 (part). Natural vibration modes of the experimental set-up with Length L_1.

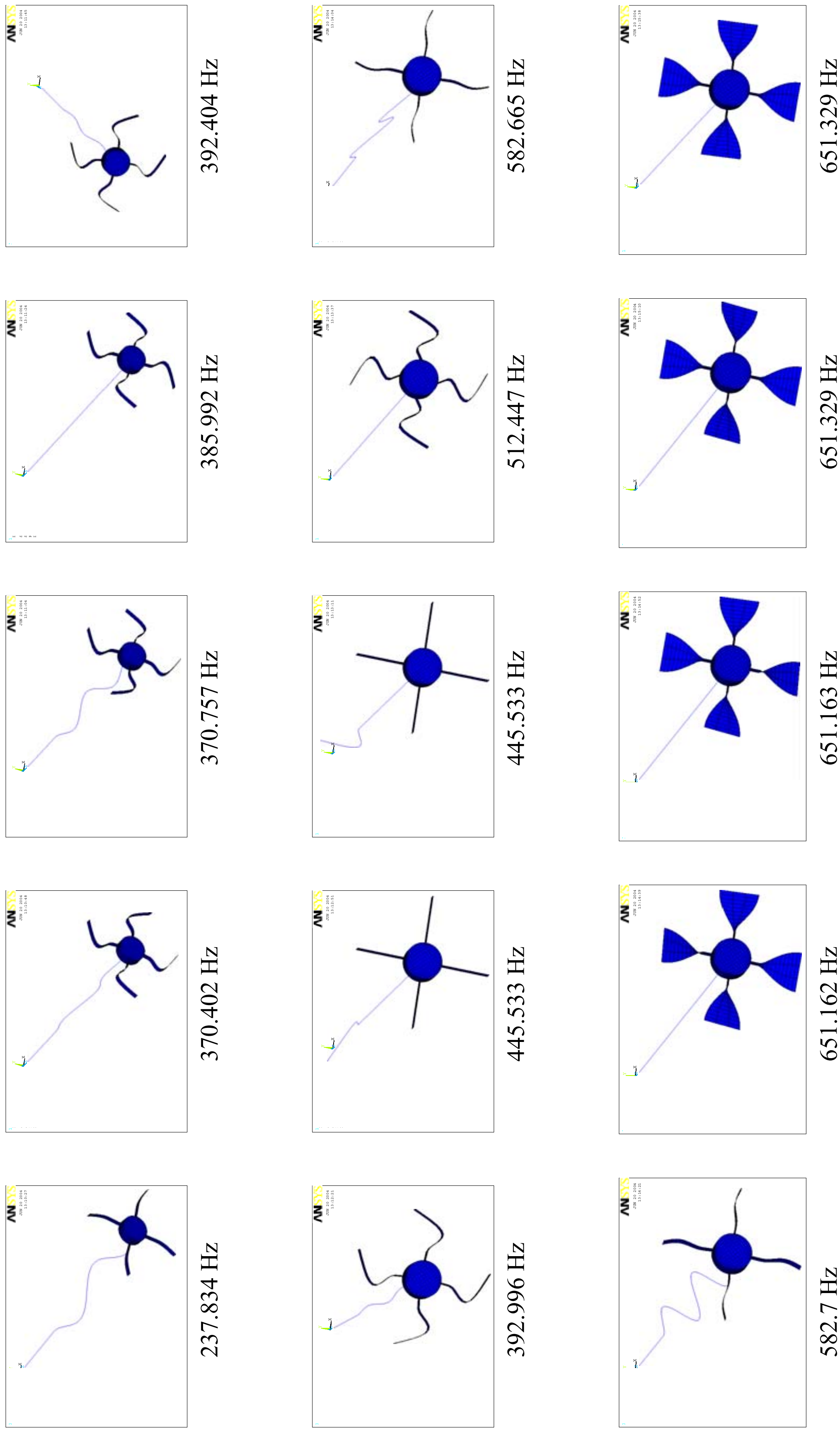

Figure 4 (cont.) Natural vibration modes of the experimental set-up with Length L_1.

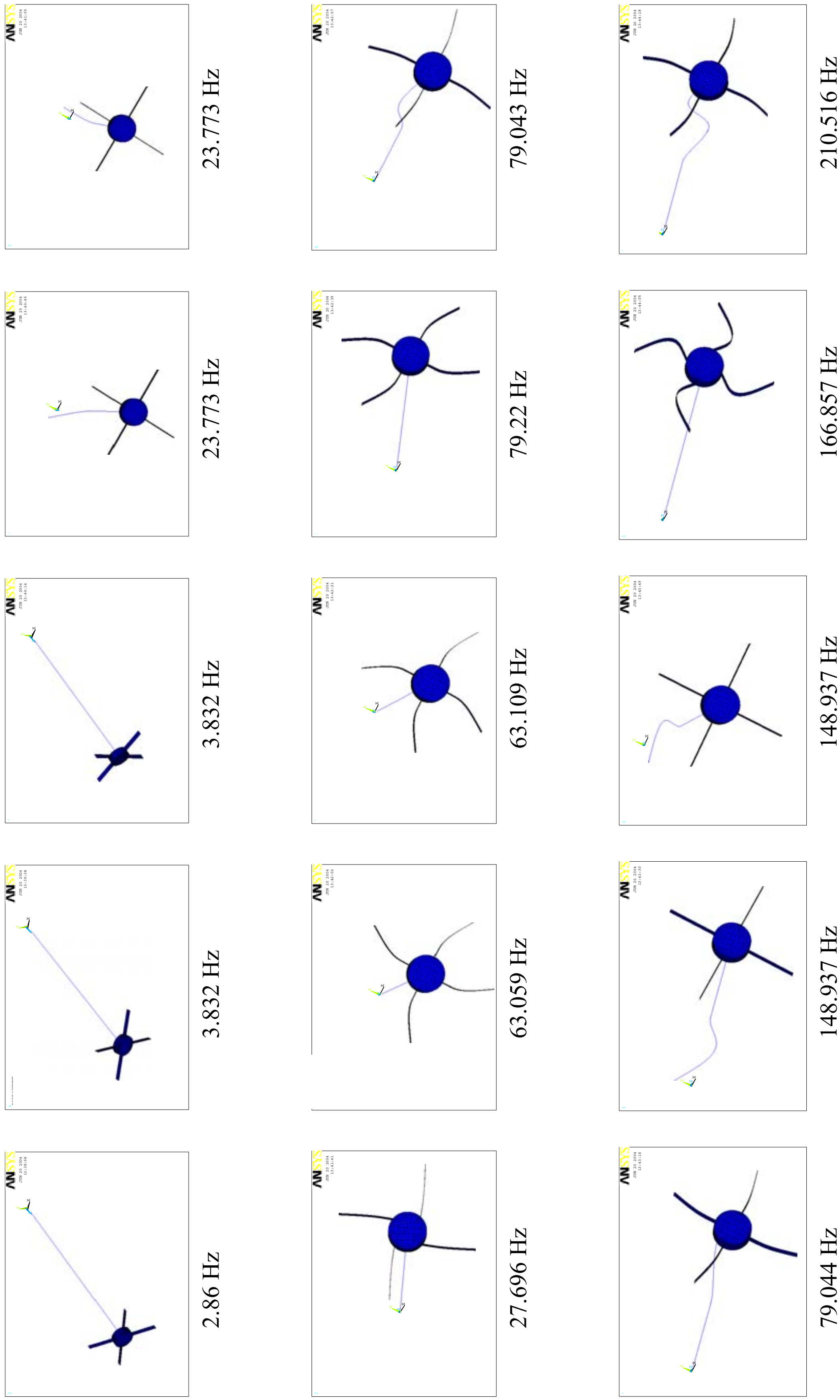

Figure 5 (part). Natural vibration modes of the experimental set-up with Length L_2.

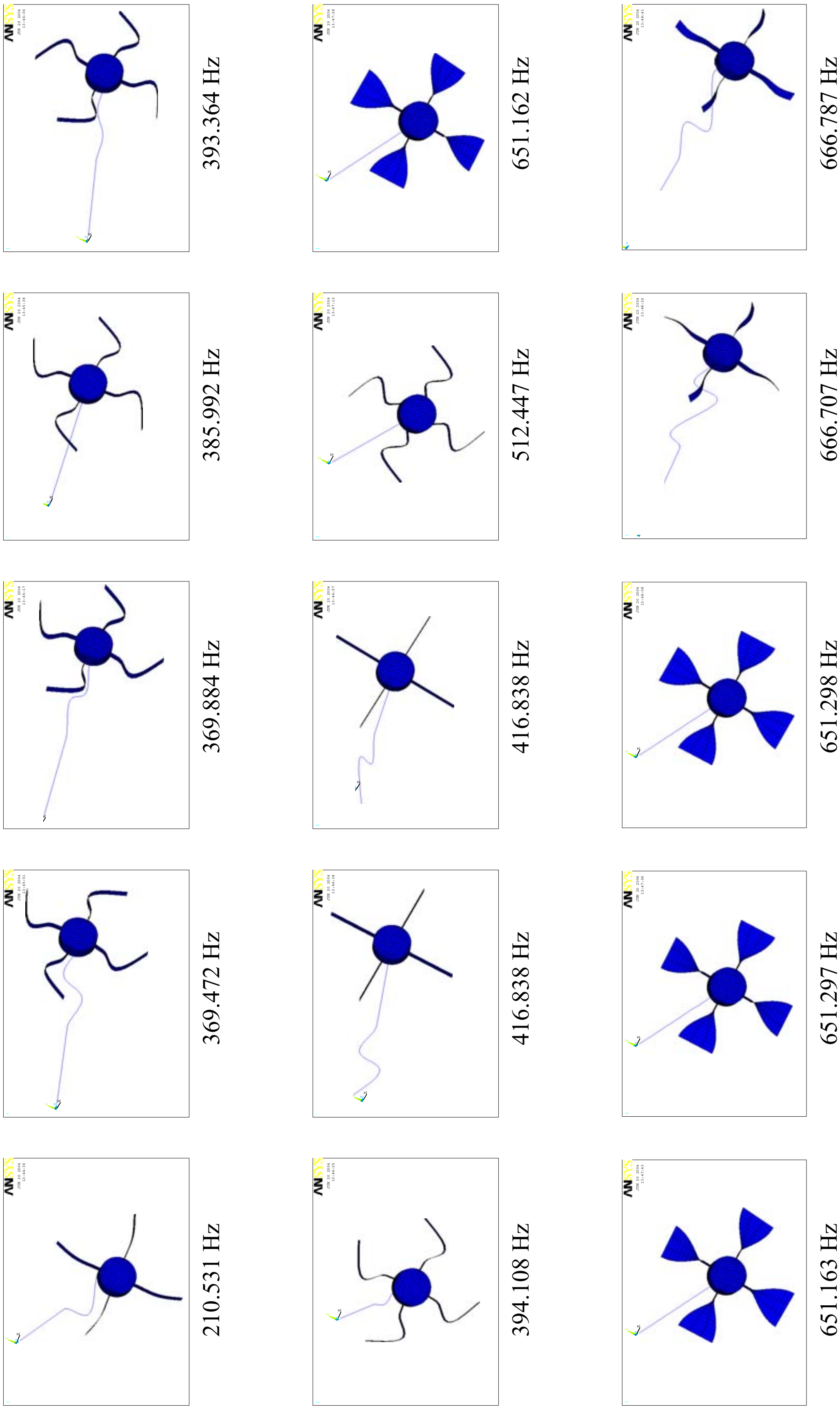

Figure 5 (cont.). Natural vibration modes of the experimental set-up with Length L_2.

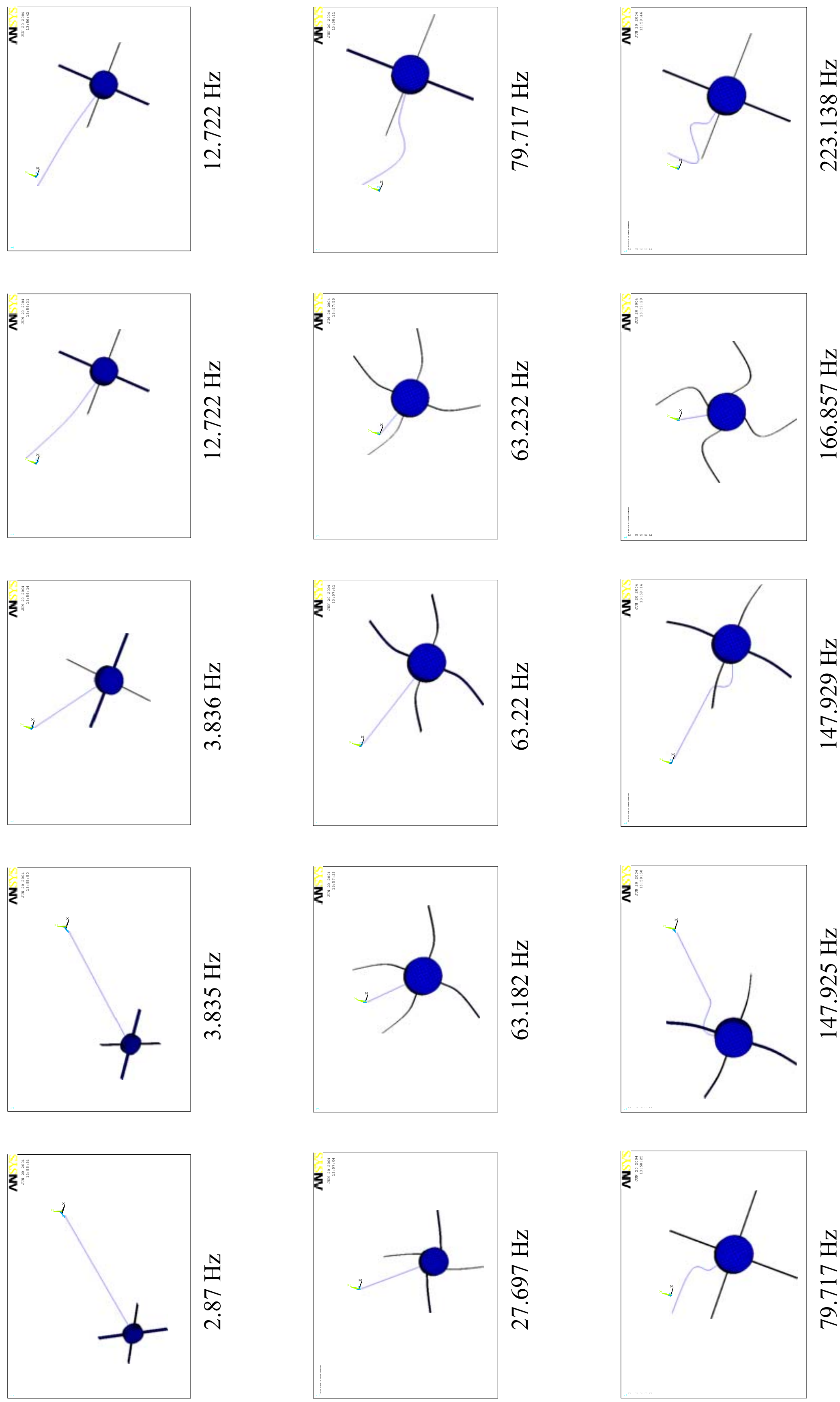

Figure 6 (part). Natural vibration modes of the experimental set-up with Length L_3.

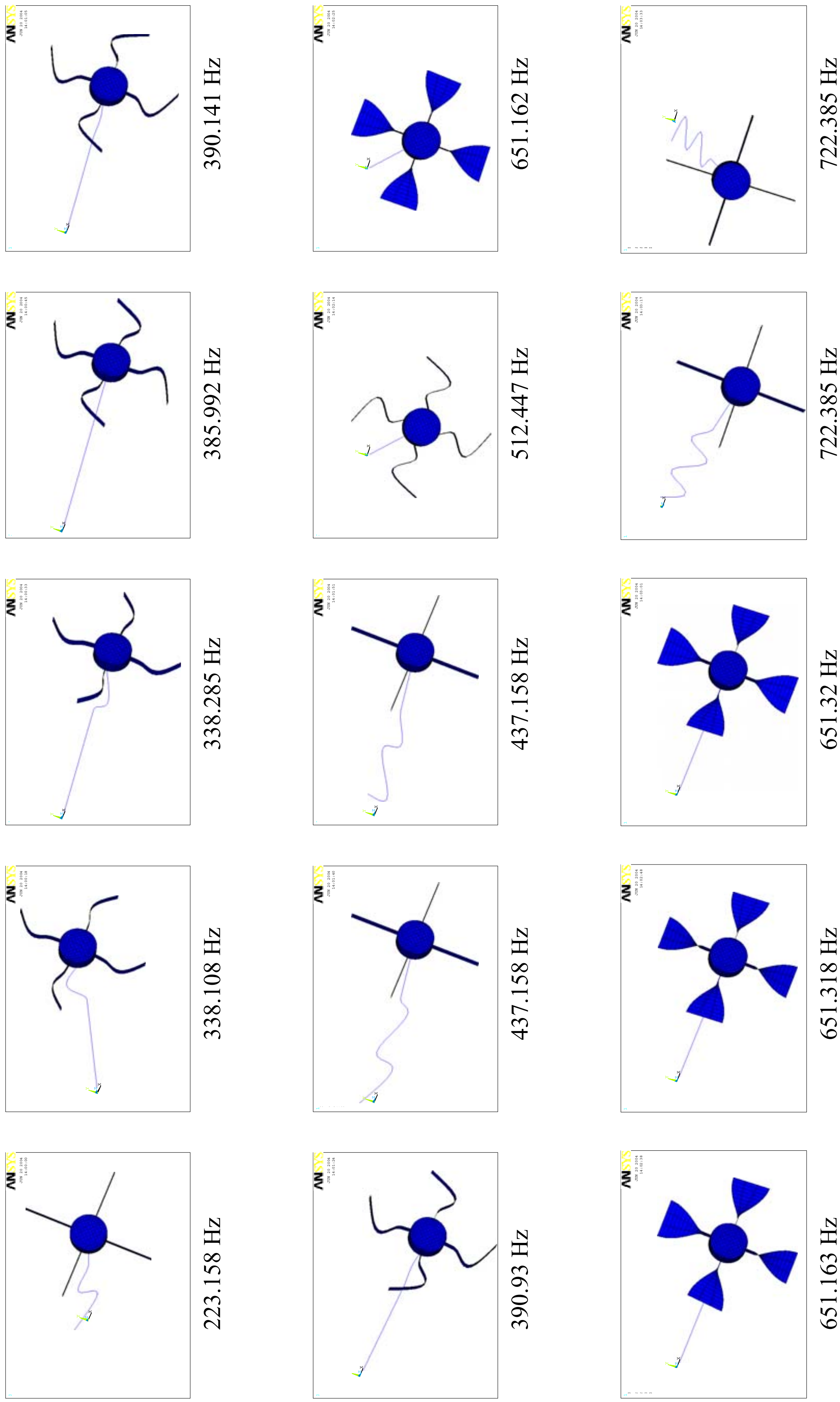

Figure 6 (cont.). Natural vibration modes of the experimental set-up with Length L_3.

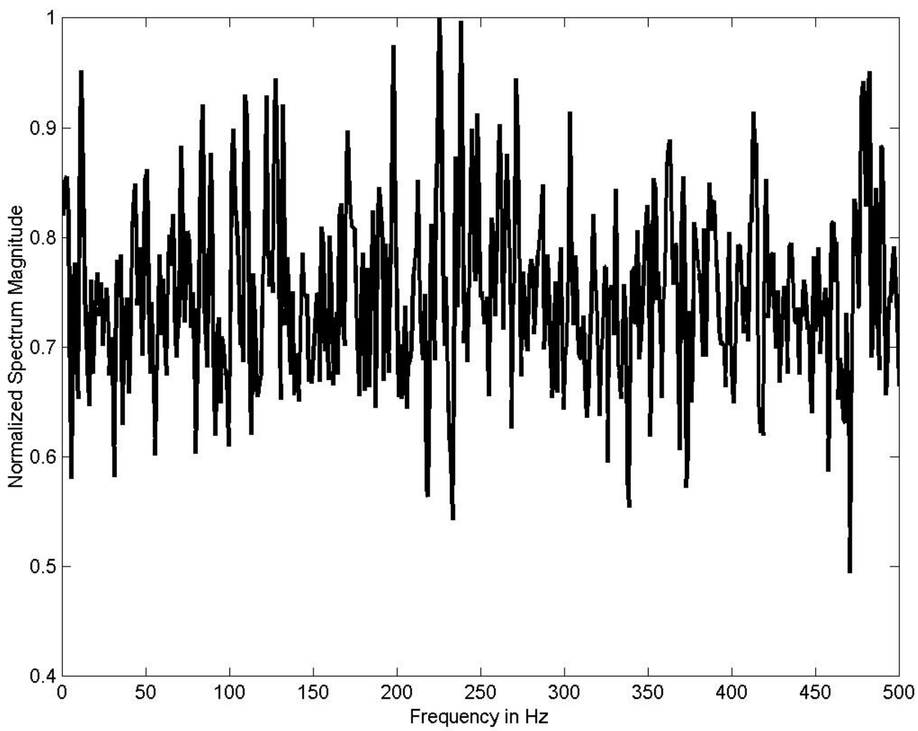

Figure 7. Blade 1 white noise random excitation frequency spectrum.

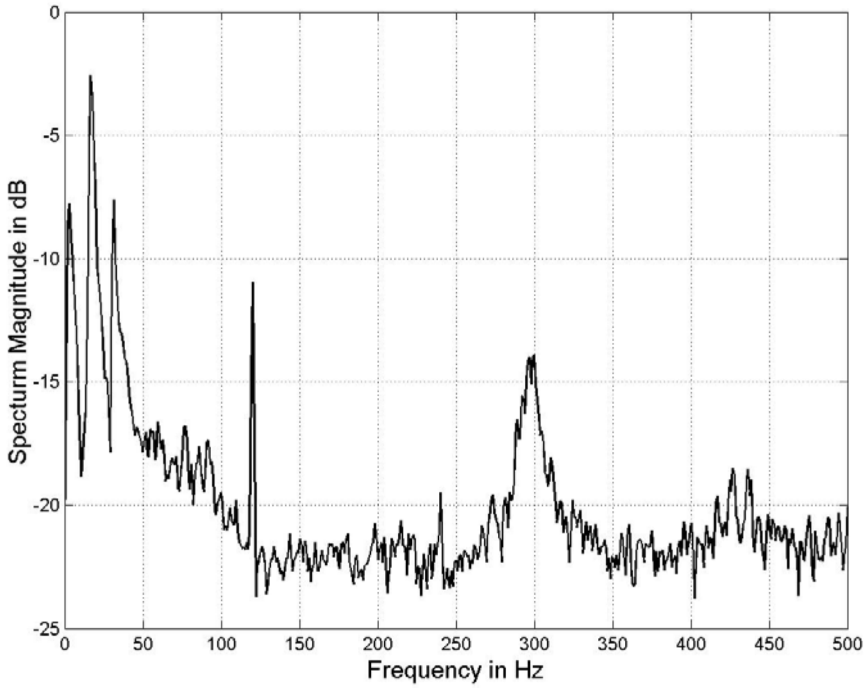

(*a*)

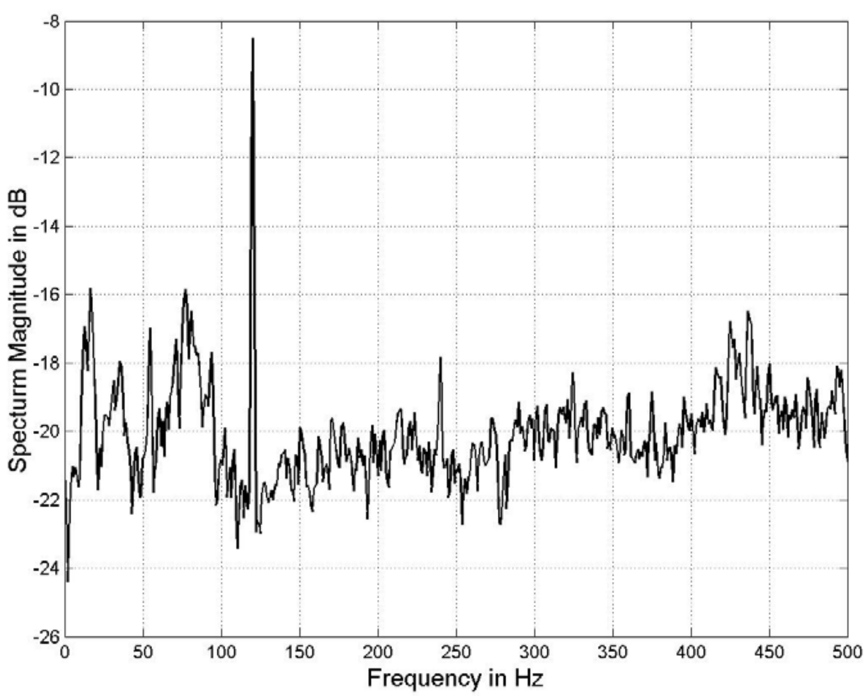

(*b*)

Figure 8. Blades strain-gages signals spectrums, shaft length L_1, (a) Blade 1 and (b) Blade 2.

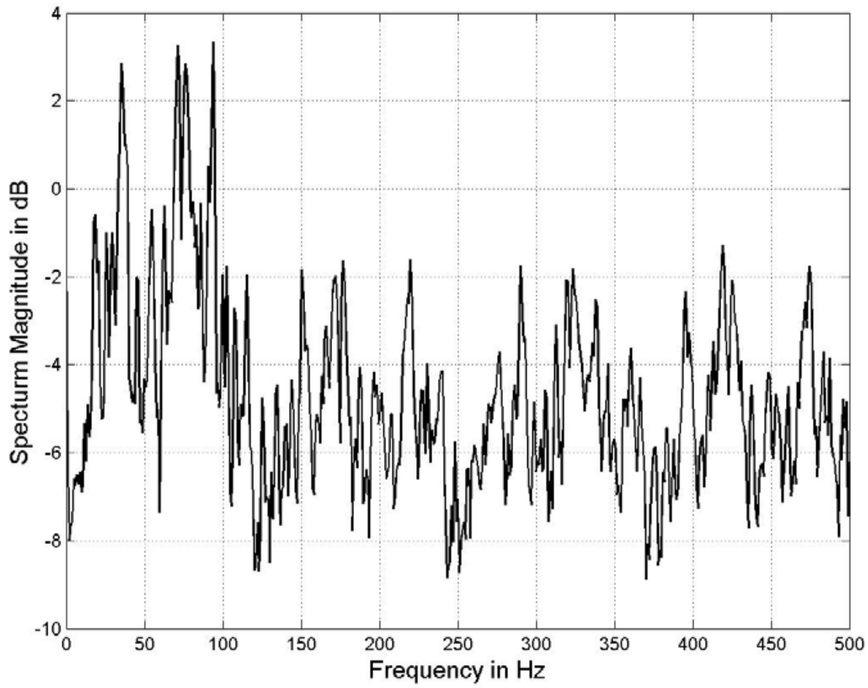

(*a*)

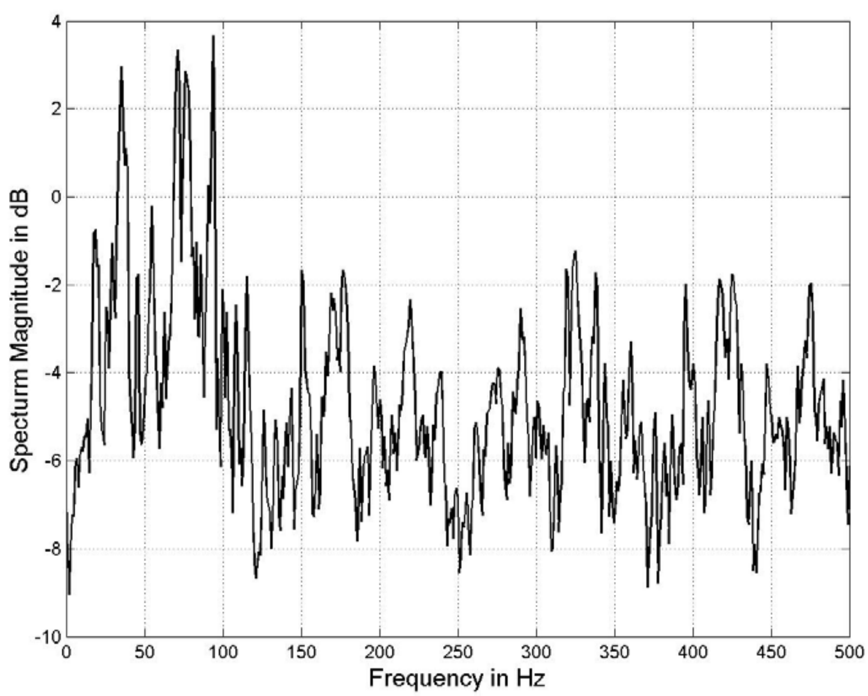

(*b*)

Figure 9: Accelerometers vibration signals spectrums, shaft length L_1,
(*a*) *Accelerometer 1 and* (*b*) *Accelerometer 2.*

(*a*)

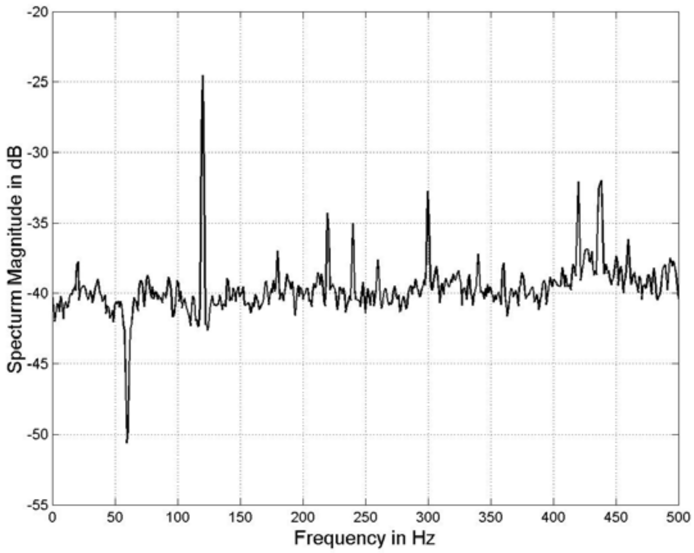

(*b*)

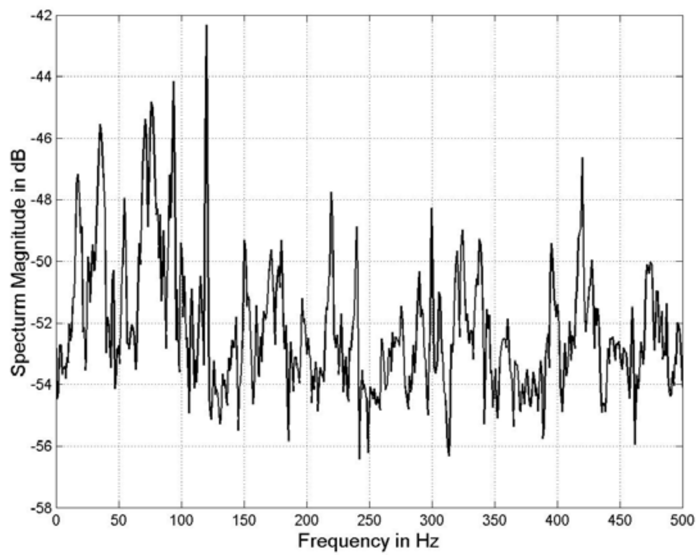

(*c*)

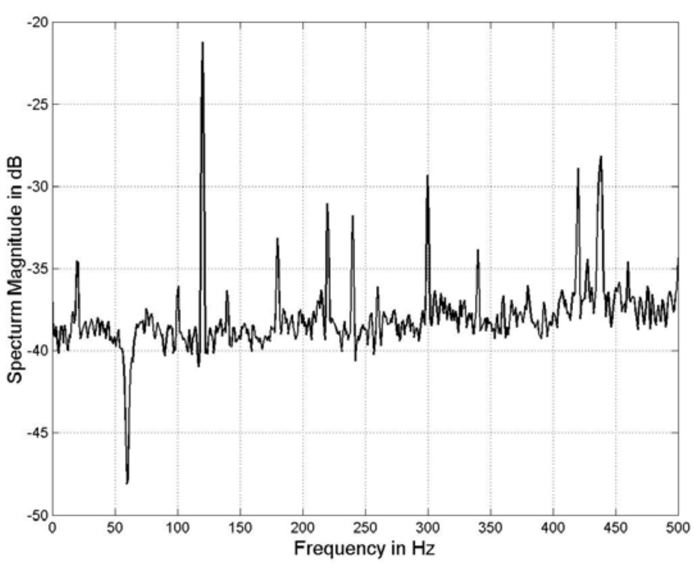

Figure 10: Shaft torsional strain gages signals spectrums, shaft length L_1,

(*a*) *Strain gage 1*, (*b*) *Strain gage 2, and* (*c*) *Strain gage 3.*

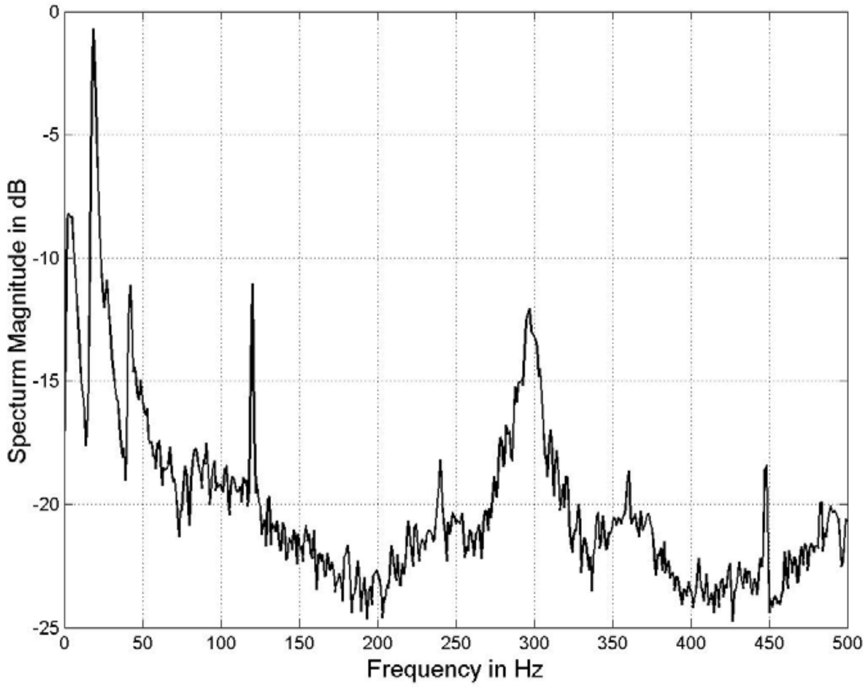

(*a*)

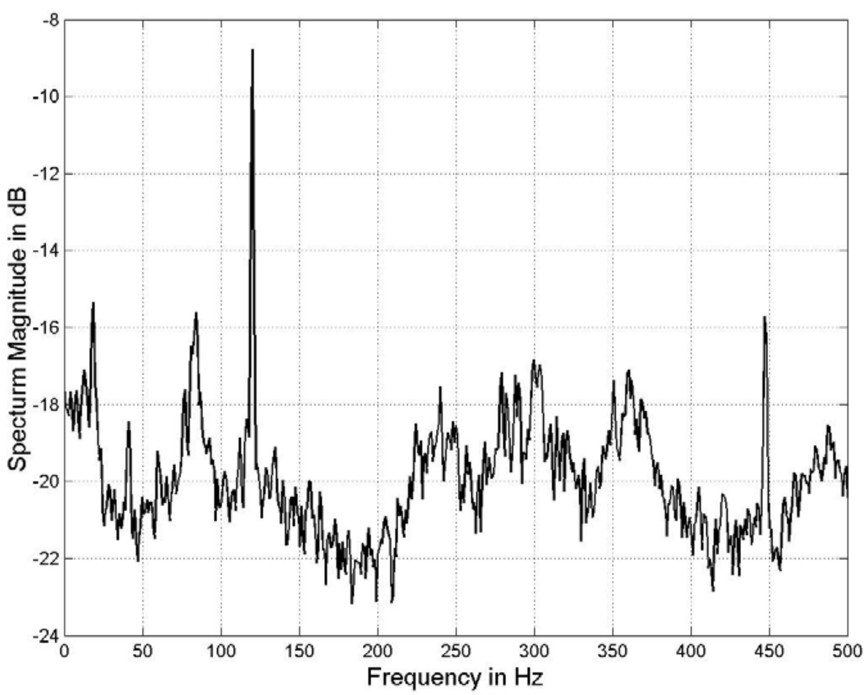

(*b*)

Figure 11. Blades strain-gages signals spectrums, shaft length L_2, (a) Blade 1 and (b) Blade 2.

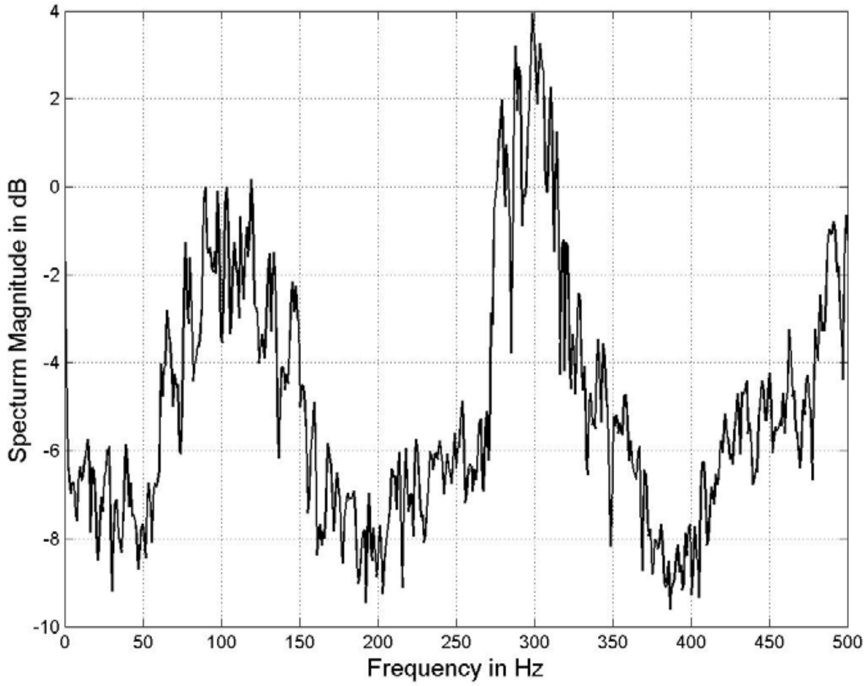

(*a*)

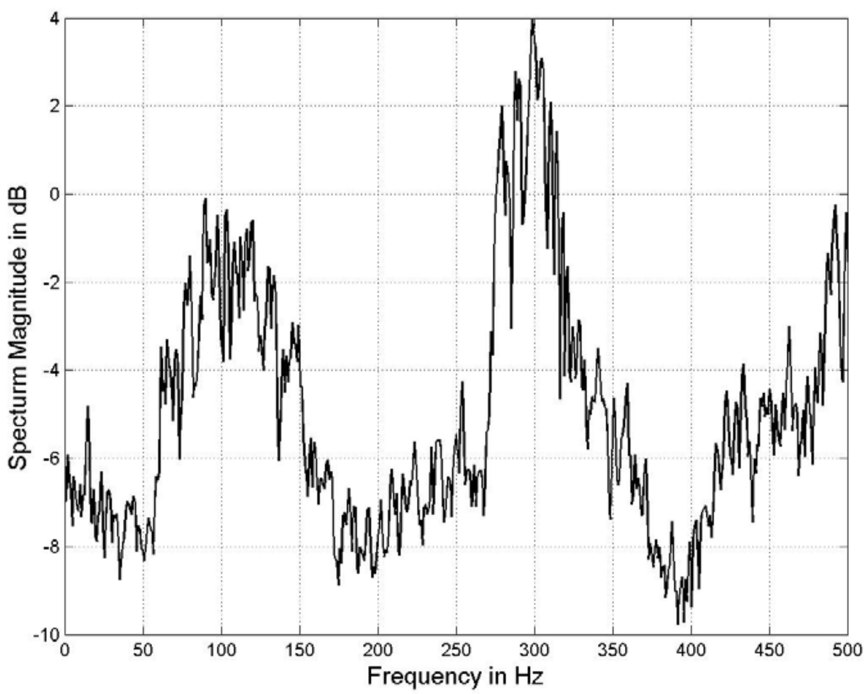

(*b*)

Figure 12. Accelerometers vibration signals spectrums, shaft length L_2,
(a) Accelerometer 1 and (b) Accelerometer 2.

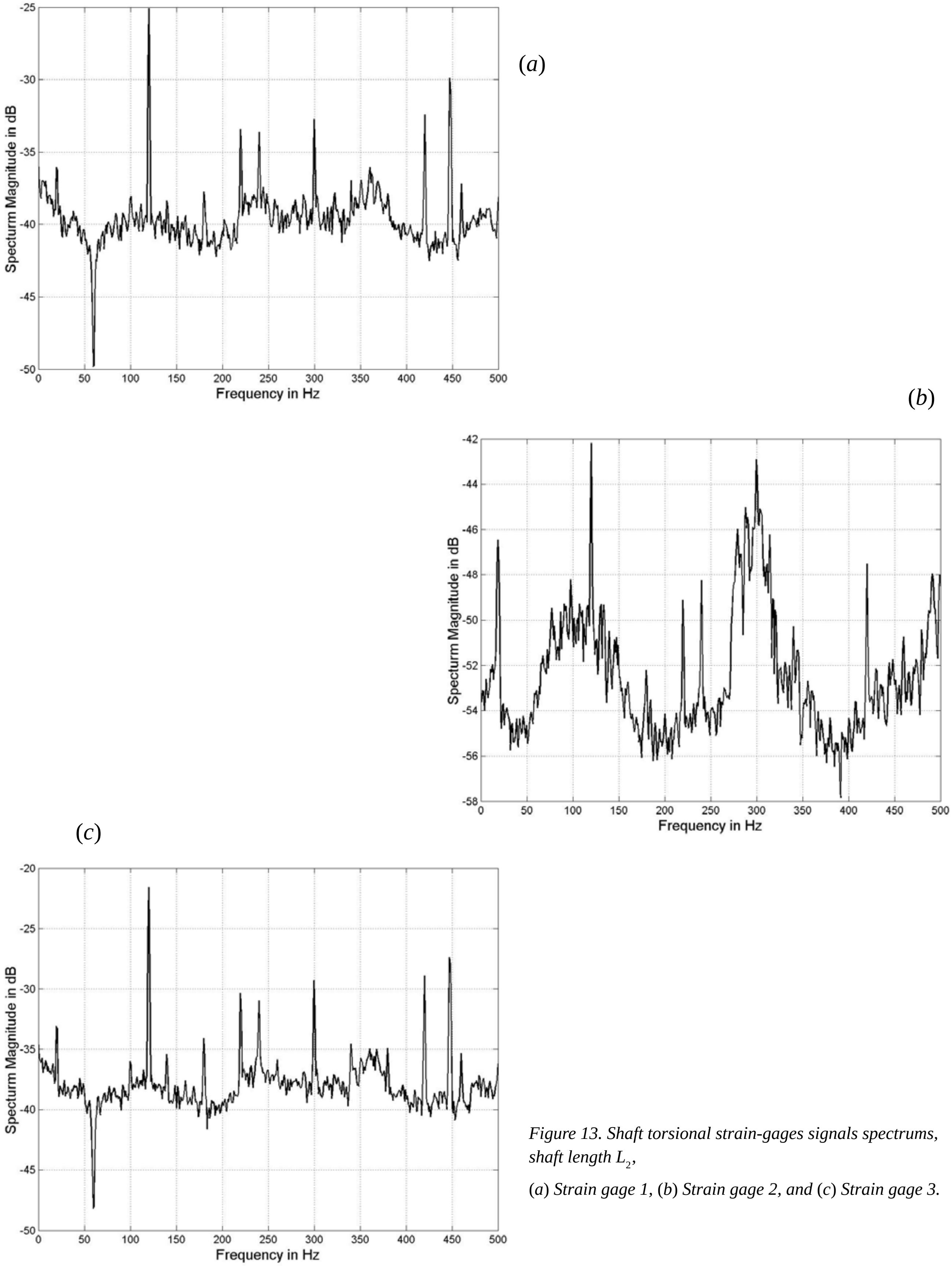

Figure 13. Shaft torsional strain-gages signals spectrums, shaft length L_2,

(*a*) *Strain gage 1,* (*b*) *Strain gage 2, and* (*c*) *Strain gage 3.*

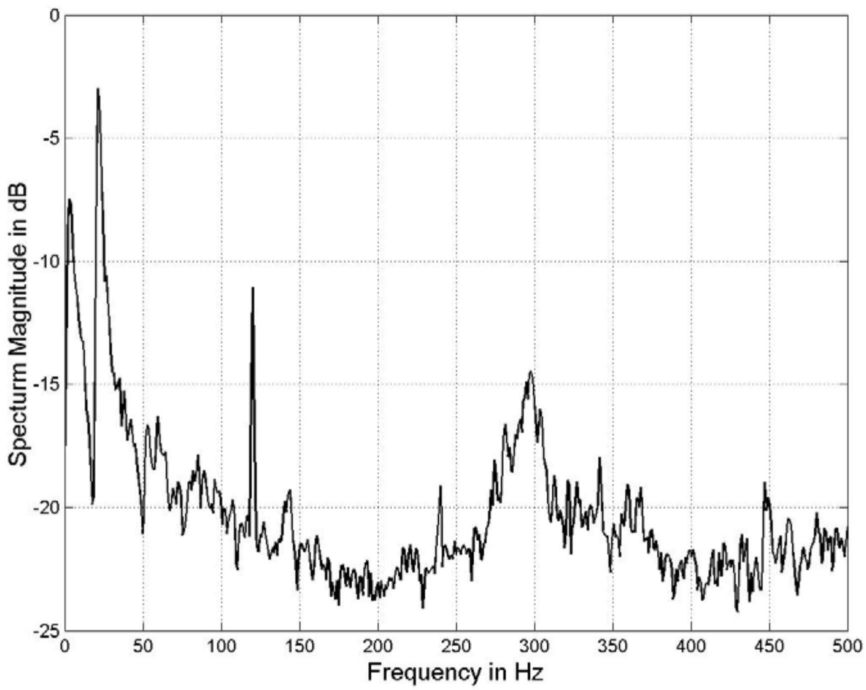

(*a*)

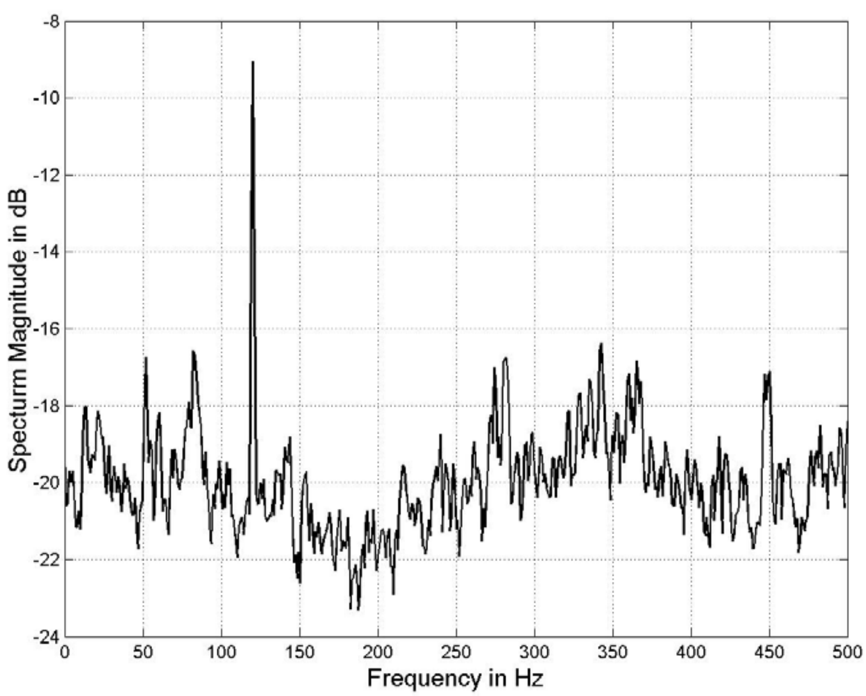

(*b*)

Figure 14. Blades strain-gages signals spectrums, shaft length L_3, (a) Blade 1 and (b) Blade 2.

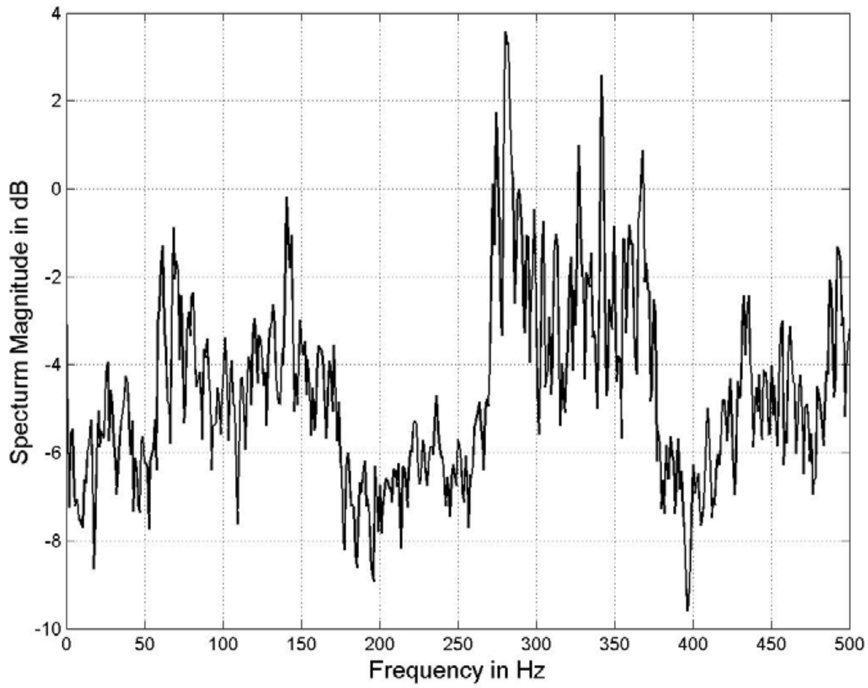

(*a*)

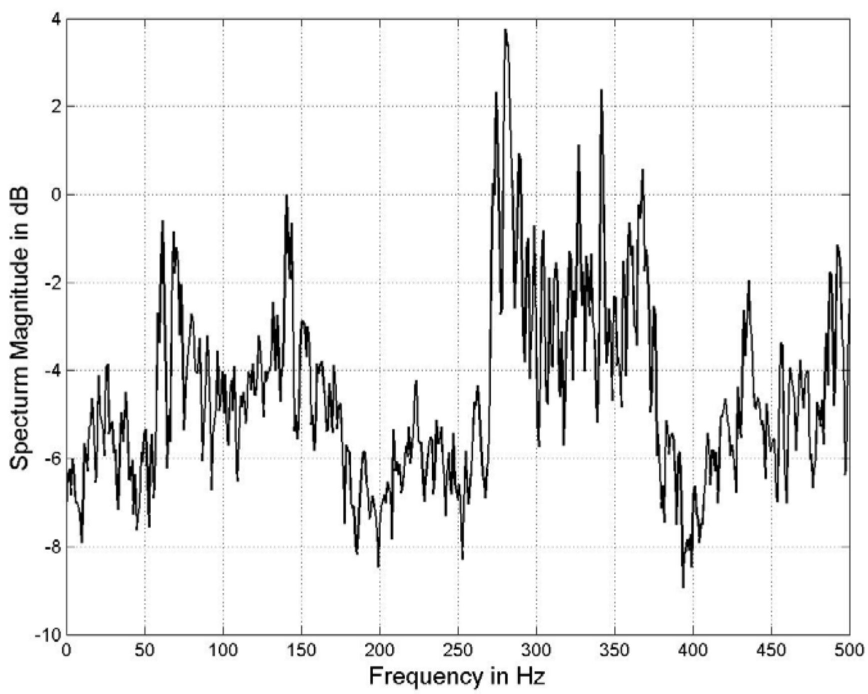

(*b*)

Figure 15. Accelerometers vibration signals spectrums, shaft length L_3,
(*a*) *Accelerometer 1 and* (*b*) *Accelerometer 2.*

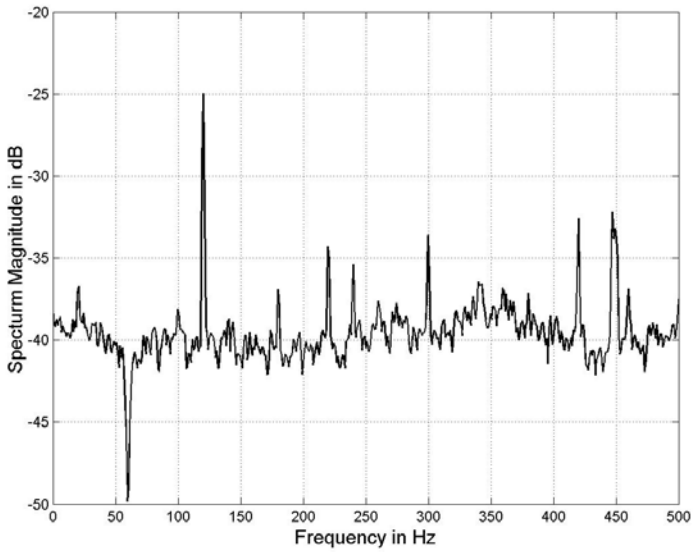

(*a*)

(*b*)

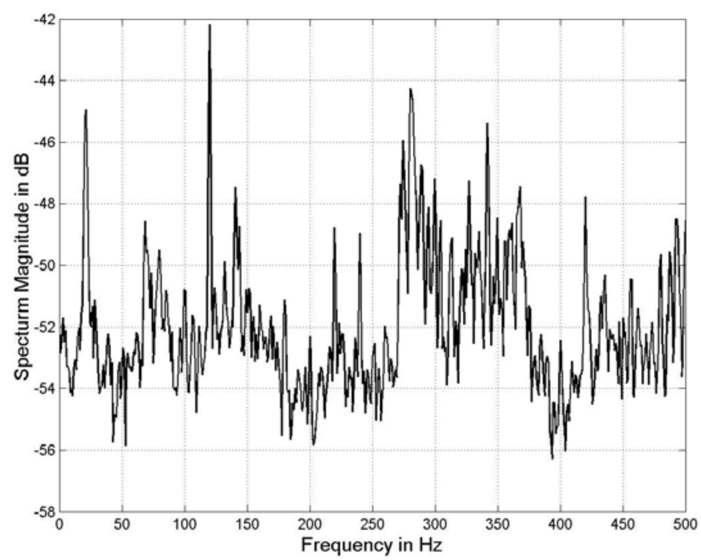

(*c*)

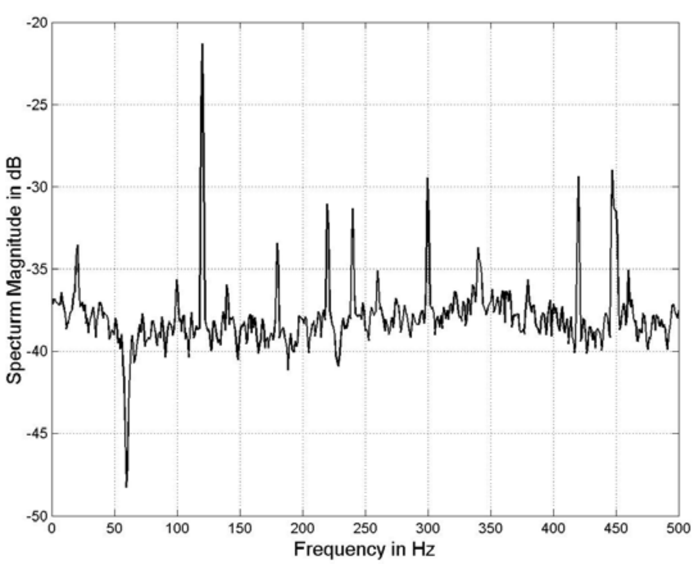

Figure 16: Shaft torsional strain gages signals spectrums, shaft length L_3,

(*a*) *Strain gage 1,* (*b*) *Strain gage 2, and* (*c*) *Strain gage 3.*

4. CONCLUSIONS

An experimental set-up for blades–shaft vibration monitoring under blade(s) random vibration excitation is used. The experimental set-up natural frequencies and mode shapes are found using the ANSYS finite element package. The blades and shaft lateral and torsional vibration are monitored using blades strain-gages, bearing accelerometers and shaft torsional strain-gages stations. The vibration signals are colleted using the LABVIEW and processed using the MATLAB package and the spectrums are analyzed and discussed. The results showed that the shaft torsional vibration measurement represent the blade(s) vibration more closely than the bearing accelerometers. In particular, the blades vibration at low frequencies corresponding to the blades–shaft torsional modes is closely represented by the shaft torsional vibration signals. The results of this study increased the confidence in using the torsional vibration measurement for blades vibration identification and shed more light on the nature of coupling between the blade bending and shaft torsional vibration that occur at low frequencies. Finally, further studies that address prototypes of machines and actual field testing are recommended.

ACKNOWLEDGMENTS

The authors acknowledge the support of King Fahd University of Petroleum (KFUPM), Dhahran, Saudi Arabia. This work is funded by KFUPM Research Office under project number ME/BLADE-VIBRATION/215.

REFERENCES

[1] W.C. Laws and A. Muszynska, "Periodic and Continuous Vibration Monitoring for Preventive/Predictive Maintenance of Rotating Machinery", *ASME Journal of Engineering for Gas Turbine and Power*, **109** (1987), pp. 159–167.

[2] J.M. Vance, *Rotor Dynamics of Turbo-Machinery*. New York: John Wiley and Sons, Inc., 1988.

[3] H.R. Simmons and A.J. Smalley, "Effective Tools for Diagnosing Elusive Turbo-Machinery Dynamics Problems in the Field", *ASME Journal of Engineering for Gas Turbines and Power*, **112** (1990), pp. 470–476.

[4] A.V. Srinivasan and D.G. Cuts, "Measurement of the Relative Vibratory Motion at the Shroud Interfaces of a Fan", *ASME Journal of Vibration, Acoustics, Stress and Reliability in Design*, **106** (1984), pp. 189–197.

[5] A.J. Scalzo, J.M. Allen, and R.J. Antos, "Analysis and Solution of a Non-Synchronous Vibration Problem in the Last Row Turbine Blade of a Large Industrial Turbine", *ASME Journal of Engineering for Gas Turbines and Power*, **108** (1986), pp. 591–598.

[6] Y.C. Fan, M.S. Ju, and Y.G. Tsuei, "Experimental Study on Vibration of a Rotating Blade", *ASME Journal of Engineering for Gas Turbines and Power*, **116** (1994), pp. 672–677.

[7] R.A. Cookson and P. Bandyopadhyay, "A Fiber-Optic Laser-Doppler Probe for Vibration Analysis of Rotating Machines", *ASME Journal of Power*, **102** (1980), pp.607–612.

[8] P. Nava, N. Paone, G.L. Rossi, and E.P. Tomasinin, "Design and Experimental Characterization of a Non-Intrusive Measurement System of Rotating Blade Vibration", *ASME Journal of Engineering for Gas Turbines and Power*, **116** (1994), pp. 657–662.

[9] A.K. Reihardt, J.R. Kadambi, and R.D. Quinn, "Laser Vibrometery Measurements of Rotating Blade Vibrations", *ASME Journal of Engineering for Gas Turbines and Power*, **117** (1995), pp. 484–488.

[10] B.O. Al-Bedoor, "Blade Vibration Measurement in Turbo-Machinery: The Current Status**",** *The Shock and Vibration Digest*, in press.

[11] K.P. Maynard and M. Trethewey, " On the Feasibility of Blade Crack Detection Through Torsional Vibration Measurements", *Proceedings of the 53rd Meeting of the Society for Machinery Failure Prevention Technology, Virginia Beach, VA*, April 19–22, 1999, pp. 451–459.

[12] K.P. Maynard, M. Lebold, C. Groover, and M. Trethewey, "Application of Double Re-Sampling to Shaft Torsional Vibration Measurement for the Detection of Blade Natural Frequencies", *Proceedings of the 54th Meeting of the Society for Machinery Failure Prevention Technology, Virginia Beach, VA*, May 1–4, 2000, pp. 87–94.

[13] K.P. Maynard and M. Trethewey, "Application of Torsional Vibration Measurement to Blade and Shaft Crack Detection in Operating Machinery", *Proceedings of the Maintenance and Reliability Conference, Gatlinburg, Tennessee*, May 6–9, 2001.

[14] A. Muszynska, P. Goldman, and D.E. Bently, "Torsional/Lateral Vibration Cross-Coupled Responses Due to Shaft Anisotropy: A New Tool in Shaft Crack Detection", *Proceedings of the IMechE Conference on Vibrations in Rotating Machinery, C 432-090, Bath, UK*, 1992, pp. 257–262.

[15] B.O. Al-Bedoor, L. Ghouti, S.A. Adewusi, Y. Al-Nassar, and M. Abdlsamad, "Experiments on the Extraction of Blade Vibration Signature from the Shaft Torsional Vibration Signals", *Journal of Quality in Maintenance Engineering,* **9**(**2**) (2003), pp.144–159.

[16] B.O. Al-Bedoor, "Model for the Extraction of Blade Vibration Signature from the Shaft Torsional Vibration Signal", *ASME Journal of Engineering for Gas Turbines and Power* (submitted).

Paper Received 25 October 2003; Revised 30 August 2004; Accepted 13 October 2004.